Journal of Molecular Catalysis A: Chemical 318 (2010) 30–35

Contents lists available at ScienceDirect

Journal of Molecular Catalysis A: Chemical

journal homepage: www.elsevier.com/locate/molcata

Polymer-anchored oxovanadium(IV) complex for the oxidation of thioanisole, styrene and ethylbenzene

Zenixole R. Tshentu[a,*], Chamunorwa Togo[b], Ryan S. Walmsley[a]

[a] Department of Chemistry, Rhodes University, Grahamstown 6140, South Africa
[b] Department of Biochemistry, Microbiology and Biotechnology, Rhodes University, Grahamstown 6140, South Africa

ARTICLE INFO

Article history:
Received 5 June 2009
Received in revised form 21 October 2009
Accepted 4 November 2009
Available online 13 November 2009

Keywords:
Polymer-anchored complex
Oxovanadium
Imidazoline
Oxidation

ABSTRACT

The ligand 2-(2′-hydroxyphenyl)-1*H*-imidazoline (Hpimin) was covalently linked to chloromethylated polystyrene (PS-Cl). This resin was then allowed to react with vanadyl sulfate to afford the polymer-anchored oxovanadium(IV) complex, PS-[VO(pimin)$_x$], which was characterised using elemental analysis, IR and AFM. This catalyst was shown to catalyse the hydrogen peroxide-based oxidation of styrene, ethylbenzene and thioanisole. A maximum conversion of ethylbenzene (30.6%) and styrene (99.9%) was obtained by using 0.025 g of PS-[VO(pimin)$_x$] and 4 equiv. of hydrogen peroxide at 80 °C after 6 h. The oxidation of thioanisole proceeded quantitatively (99.6%) within 4 h, with 0.025 g of PS-[VO(pimin)$_x$], at room temperature with 2 equiv. of hydrogen peroxide. At the steady state, the main products from the oxidation of the various substrates were benzaldehyde (57.6%) > 1-phenylethane-1,2-diol (16.2%) > benzoic acid (7.1%) > styrene oxide (3.1%) for styrene; acetophenone (20.5%) > benzaldehyde (2.7%) for ethylbenzene; and methyl phenyl sulfoxide (67.4%) > methyl phenyl sulfone (31.9%) for thioanisole.

1. Introduction

The simple separation and recyclability [1] of heterogeneous catalysts provides an attractive option for laboratory scale synthesis, while the ability to easily apply these catalysts to industry in the form of packed or fluidised bed columns [2] provides yet another incentive. The use of polymeric supports for the immobilisation of metal catalysts has been thoroughly studied [1,3,4] and remains an exciting area of research with potential for further discoveries [5]. The catalytic properties of oxovanadium compounds lead them to be of particular interest in this regard [6].

The ever increasing environmental concerns present a motive for replacing toxic oxidising agents such as chromium and permanganate-based agents with 'environmentally friendly' varieties such as molecular oxygen and hydrogen peroxide, which generate water as the only by-product [7,8]. Alkenes, sulfides and alcohols have been oxidised with both air oxygen [9,10] and excited singlet oxygen [11,12] through metal-based activations. Hydrogen peroxide has also become increasingly popular due to its low cost and availability [5] and has been used for a wide range of reactions including the oxidation of sulfides, alkenes and alkanes [13].

Herein, we describe the preparation, characterisation and catalytic evaluation of a heterogeneous oxovanadium(IV) catalyst. The ligand 2-(2′-hydroxyphenyl)-1*H*-imidazoline was covalently linked to chloromethylated polystyrene, and the resultant cream-coloured beads were allowed to react with vanadyl sulfate to form the light green polymer-anchored complex. The beads were characterised by microanalysis, infrared spectroscopy and atomic force microscopy. The catalytic activity of the oxovanadium(IV) complex was investigated for the oxidation of thioanisole, styrene and ethylbenzene by using hydrogen peroxide as the oxidant. The reaction progress was monitored by gas chromatography.

2. Experimental

2.1. Materials

Thioanisole, ethylbenzene, styrene, ethylenediamine, vanadyl sulfate hydrate and Merrifield polymer crosslinked with divinylbenzene (5.5% crosslinked, ~5.5 mmol Cl/g resin and 16–50 mesh) were purchased from Aldrich Chemical Company and used without further purification. All other chemicals and solvents were of reagent grade.

2.2. Instrumentation

The infrared spectra were recorded on a PerkinElmer 2000 FTIR spectrometer in the mid-IR range (4000–400 cm^{-1}) as KBr pellets. ^{1}H and ^{13}C NMR spectra were recorded on a Bruker AMX 400 NMR MHz spectrometer and reported relative to tetramethylsi-

* Corresponding author. Tel.: +27 46603 8846; fax: +27 46622 5109.
E-mail address: z.tshentu@ru.ac.za (Z.R. Tshentu).

1381-1169/$ – see front matter © 2009 Elsevier B.V. All rights reserved.
doi:10.1016/j.molcata.2009.11.004

lane (δ 0.00). Electronic spectra were recorded on a Varian Cary 500 Scan UV–vis spectrophotometer using 1 cm quartz cells and dimethylsulfoxide as the solvent. The vanadium content of beads was determined by using a Thermo Electron (iCAP 6000 Series) inductively coupled plasma (ICP) spectrometer equipped with an OES detector. The wavelengths 290.88 nm, 292.40 nm, 309.31 nm and 311.07 nm were chosen and triplicate analyses were performed at each wavelength. Catalysed reactions were monitored by using an Agilent 6820 gas chromatograph (GC), fitted with a flame ionization detector (FID) and a ZB-5MSi capillary column (30 m × 0.25 mm × 0.25 μm). Mass spectra were obtained by using a Thermo-Finnigan GC–MS fitted with an electron impact ionization mass selective detector. Atomic force microscopy (AFM) imaging was performed using a CP-11 scanning probe microscope from Veeco Instruments in non-contact mode at a scan rate of 2 Hz by using an MP11123 cantilever. Microanalysis was carried out by using a Vario Elementar Microcube ELIII.

2.3. Preparative work

2.3.1. 2-(2'-Hydroxyphenyl)-1H-imidazoline (Hpimin)

Methyl salicylate (18.4 g, 0.12 mol) was added to an excess of ethylenediamine (32 g, 0.53 mol) in a conical flask and placed in a conventional microwave (7 min, 180 W) with intermittent stirring. Starting materials were removed by vacuum distillation (7×10^{-3} mbar at 160 °C) to afford a crude solid product which was then purified by digestion from a large volume of chloroform. Yield: 78.1%. ^{1}H NMR (400 MHz, DMSO-d_6): δ 3.71 (s, 4H, CH_2CH_2), 6.69 (t, 1H, Ar-H) 6.77, (d, 1H, Ar-H), 7.27 (t, 1H, Ar-H), 7.56 (d, 1H, Ar-H). ^{13}C NMR (400 MHz, DMSO-d_6): δ 46.5, 110.2, 115.5, 118.4, 127.2, 132.7, 163.5, 166.1; Anal. Calcd for $C_9H_{10}N_2O$ (Found): C, 66.65% (66.68%); H, 6.21% (6.20%); N, 17.27% (16.98%).

2.3.2. [VO(pimin)$_2$]

To a solution of Hpimin (0.25 g, 1.5 mmol) in 5 mL methanol was added vanadyl sulfate (0.15 g, 0.7 mmol) dissolved in 5 mL water. The mixture was stirred at room temperature to afford a green precipitate within 10 min. The reaction was allowed to proceed for further 2 h to reach completion. The solid was collected by filtration and washed with water followed by cold methanol, and then finally dried in an oven at 100 °C. Yield: 57%. Anal. Calcd for $C_{18}H_{18}N_4O_3V$ (Found): C, 55.53% (55.43%); H, 4.66% (4.74%); N, 14.39% (14.21%).

2.3.3. Polymer-anchored ligand (PS-pimin)

Chloromethylated polystyrene (1.0 g, 5.5 mmol Cl) was allowed to swell in DMF (15 mL) overnight. To this was added Hpimin (0.93 g, 5.7 mmol) followed by a solution of triethlyamine (1.25 g) in ethylacetate (30 mL). The reaction mixture was then heated and stirred under reflux for 9 h. Following this, the cream-coloured beads were allowed to cool and then filtered and washed with hot DMF followed by ethanol. The beads were dried in the oven at 60 °C. Due to some degradation from mechanical stirring the beads were first passed through sieves of various mesh sizes such that only the largest beads remained (>15 mesh). Anal. Found: C, 69.80%; H, 6.93%; N, 5.79%.

2.3.4. Polymer-anchored vanadium complex (PS-[VO(pimin)$_x$])

PS-pimin (0.5 g) was allowed to swell in DMF for 2 h. A DMF solution of vanadyl sulfate (0.6 g, 2.75 mmol) was added to the above mixture, which was stirred and heated at 90 °C for 8 h. The green beads were collected by filtration, rinsed with warm DMF and methanol and then dried in the oven at 60 °C. Anal. Found: C, 62.12%; H, 5.99%; N, 4.63%; S, 2.11%; V, 4.70%.

2.4. Catalytic activity studies

In a typical catalytic oxidation experiment, 20 mL of acetonitrile was added to a 100 mL round bottom flask fitted with a glass condenser. The temperature of the oil bath was regulated to ±1 °C by using an external temperature probe. The stirring rate was kept constant at 300 rpm for all reactions. Then, styrene (1.04 g, 10 mmol), ethylbenzene (1.06 g, 10 mmol) or thioanisole (1.24 g, 10 mmol) was added followed by the required moles of hydrogen peroxide. Immediately after the addition of hydrogen peroxide, the catalyst was added and this was considered the start of the reaction. The reaction progress was monitored by gas chromatography at specific time intervals.

3. Results and discussion

3.1. Synthesis and general considerations

The synthesis of the ligand (Hpimin) has been carried out before [14]. Our synthesis, however, employs an efficient microwave method with a short reaction time of 7 min and improved yield of 78%. The alkylation of Hpimin with chloromethylated polystyrene under the specified conditions might occur at different positions (see Scheme 1) as also acknowledged recently by Maurya et al. [15].

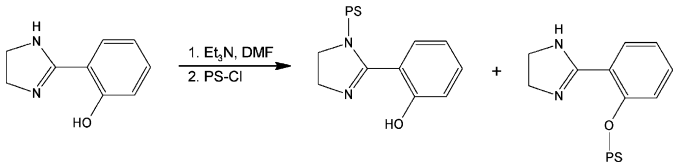

Scheme 1. Expected products for the alkylation of Hpimin.

As a result of the above, the subsequent complex formation step may be expected to yield an oxovanadium(IV) complex with a different stereochemistry to that of the neat square pyramidal complex, [VO(pimin)$_2$]. In [VO(pimin)$_2$], Hpimin coordinates as a bidentate phenolate ligand via the imidazoline nitrogen and the deprotonated phenolic group to form the five coordinate complex.

3.2. Spectral characterisation

The infrared spectrum of chloromethylated polystyrene (PS-Cl) shows a band at 670 cm^{-1} corresponding to the ν(C–Cl) vibration [16], and the attachment of Hpimin to polystyrene was confirmed by its disappearance and the appearance of a new band at 1615 cm^{-1} corresponding to the ν(C=N) vibration. In the spectrum of the free ligand, a medium and broad band for the stretching frequency of the hydrogen bonded O–H appears at 2695 cm^{-1} [17] but disappears in the spectrum of PS-pimin. This along with the appearance of the ν(C–O–C) band at 1233 cm^{-1} suggests that alkylation occurs predominantly *via* the hydroxyl group [14]. The selected infrared data is listed in Table 1.

A medium intensity band at 992 cm^{-1} confirms the presence of the oxovanadium unit [15]. Interestingly, this stretching frequency is markedly different from that of the non-polymer-bound complex, [VO(pimin)$_2$], once again suggesting that the stereochemistry is different, which agrees well with our proposal that alkylation occurs *via* the hydroxyl group of the ligand. This was again corroborated by the microanalysis results which show a significant amount of sulfur (2.11% from sulfate) as well as a V/S ratio of approximately 1:1.3, indicating that a cationic species of oxovanadium(IV) forms within the polymer. Furthermore, a V/N ratio in the polymer of 1:3.6 indicates the possibility of vanadyl bound to two imidazoline units. It is, however, not possible to characterise the exact nature

Table 1
Selected infrared bands and the colours of the compounds.

Compound	Colour	IR bands (cm^{-1})			
		ν(C–Cl)	ν(C=N)	ν(O–H)	ν(V=O)
Hpimin	Cream	–	1618	2695	–
PS-Cl	White	670	–	–	–
PS-pimin	Cream	–	1615	–	–
PS-[VO(pimin)$_x$]	Green	–	1610	–	992
[VO(pimin)$_2$]	Green	–	1609	–	932

of the complex species within the polymer. The coordination of pimin to oxovanadium(IV) is shown by the decrease in ν(C=N) from 1618 cm^{-1} in the free ligand to 1609 cm^{-1} and 1610 cm^{-1} in PS-[VO(pimin)$_x$] and [VO(pimin)$_2$], respectively. The ν(C–O) for Hpimin was observed at 1269 cm^{-1} and shifted to 1255 cm^{-1} upon coordination in the non-polymer-bound complex, [VO(pimin)$_2$].

The electronic spectrum of the neat complex shows three bands at 411 nm ($a_1^* \leftarrow b_2$), 549 nm ($b_1^* \leftarrow b_2$) and 617 nm ($e_\pi^* \leftarrow b_2$) typical of the five-coordinate, square pyramidal geometry corresponding to the neutral [VO(pimin)$_2$] [18,19].

3.3. Atomic force microscopy

The atomic force micrographs for the single beads of PS-Cl, PS-pimin, PS-[VO(pimin)$_x$] and the recovered PS-[VO(pimin)$_x$] showed the morphological changes of the surfaces of the beads after the various synthetic steps. Additionally, the extent of degradation of the polymer after a catalytic cycle was investigated.

The results show an increase in surface roughness from 4.47 nm in PS-Cl to 6.14 nm in PS-pimin, and a decrease to 5.06 nm upon forming the PS-[VO(pimin)$_x$] signifying perhaps the rigidity of the ligands at the surface upon coordination to vanadyl. The surface roughness of the beads recovered from a room temperature reaction for the oxidation of thioanisole with peroxide is 104.7 nm. It is apparent that the peroxide plays a significant role in the degradation of the beads at the surfaces despite the fact that they still exhibit catalytic activity upon recycling. The AFM images are shown in Appendix A.

3.4. Catalytic activity

The polymer-anchored complex, PS-[VO(pimin)$_x$], and its geometrically non-equivalent homogeneous counterpart, [VO(pimin)$_2$], were investigated for their catalytic efficiency for the oxidation of thioanisole, styrene and alkylbenzene using acetonitrile as a solvent and 30% hydrogen peroxide as the oxidant.

3.4.1. Oxidation of thioanisole

In this study thioanisole is oxidised to give the corresponding methyl phenyl sulfoxide and methyl phenyl sulfone, which are identified by GC and GC–MS data, as shown in Scheme 2.

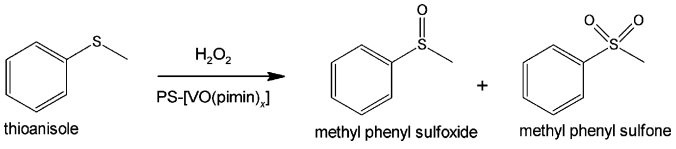

Scheme 2. Oxidation products for thioanisole.

To optimise the reaction conditions, the effects of the amount of catalyst as well as the effect of temperature were investigated. According to the literature [20], the oxidation of sulfides invariably reaches a maximum conversion at a 2:1 peroxide-to-sulfide ratio and even less, and therefore in our study this ratio was kept constant. The effect of the amount of catalyst, in the range 0.0–0.035 g, on the rate of oxidation was studied as a function of time and the results are shown in Fig. 1. For a fixed amount of thioanisole (1.24 g, 10 mmol) in 20 mL of acetonitrile and 30% H_2O_2 (20 mmol) at room temperature, the rate of the oxidation reaction is fast for the highest catalyst amount of 0.035 g reaching 98.9% conversion within 1 h. However, the 0.025 g amount of catalyst results in maximum conversion of 99.6% within 3 h at room temperature, making this a catalytically relevant amount.

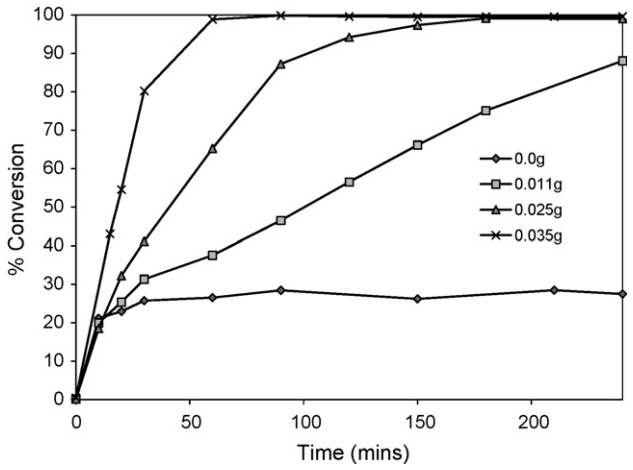

Fig. 1. The effect of catalyst amount on thioanisole oxidation. Reaction conditions: thioanisole (1.24 g, 10 mmol), 30% H_2O_2 (20 mmol), acetonitrile (20 mL) and room temperature (RT).

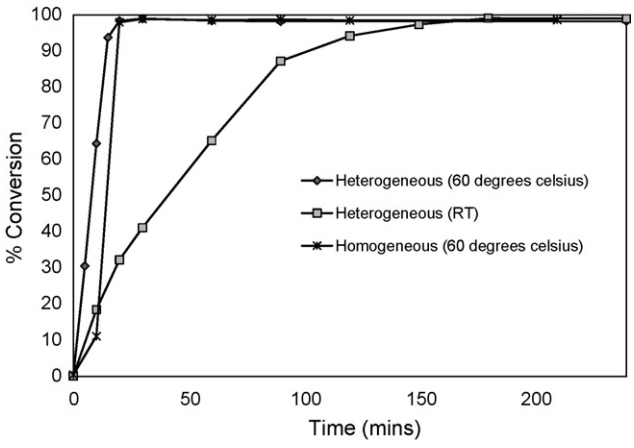

Fig. 2. Effect of temperature on oxidation of thioanisole (1.24 g) using 0.025 g of catalyst, and the comparison with neat complex (0.0090 g) at 60 °C.

The rate of reaction improves drastically at higher temperatures, reaching maximum conversion of 98.3% within 20 min when 0.025 g of catalyst is used, and compares well with its homogeneous counterpart at 60 °C (see Fig. 2). The amount of [VO(pimin)$_2$] (0.0090 g) was reconciled by determining the amount of vanadium in 0.025 g of the beads. This was done by placing 0.025 g of catalyst in 10 mL of TraceSelect nitric acid (69%) at 40 °C overnight to leach out vanadium. This acid-leached solution was then diluted with deionized, distilled water to 100 mL, and analysed by ICP-OES.

The initial rate for the oxidation of thioanisole increases rapidly due to the formation of methyl phenyl sulfoxide, with little conversion of the sulfoxide to sulfone. The kinetics follows those of consecutive reactions, with the sulfoxide being converted to the sulfone form. Fig. 3 shows the selectivities or the progress of the consecutive reactions with time.

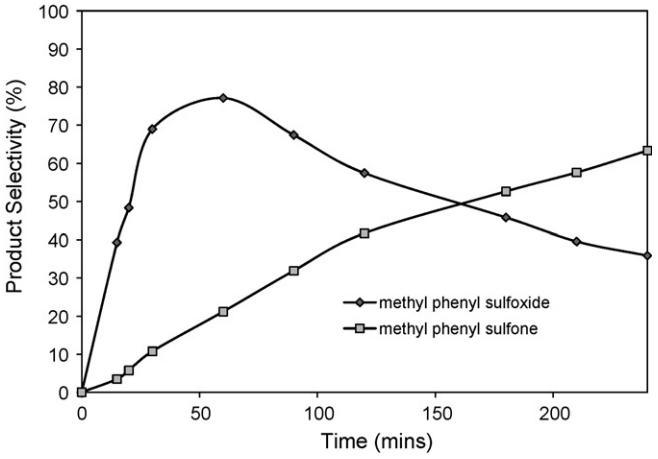

Fig. 3. Product selectivity for the oxidation of thioanisole. Reaction conditions: 1.24 g of thioanisole, 0.035 g of catalyst, 2 equiv. of H_2O_2, room temperature and 20 mL of acetonitrile.

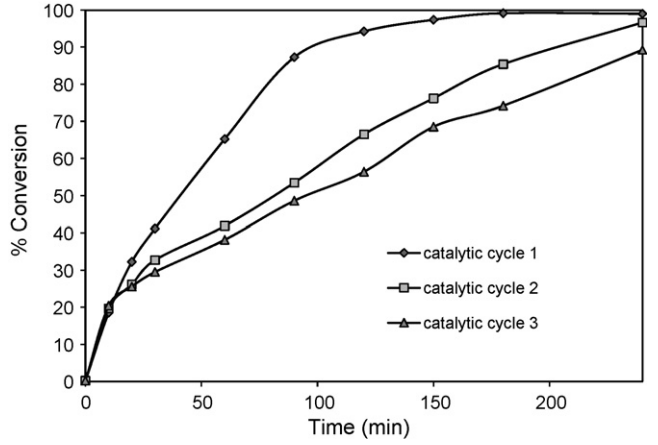

Fig. 4. The recyclability of PS-[VO(pimin)$_x$] in the oxidation of thioanisole. Reaction conditions: 1.24 g of thioanisole, 0.025 g of catalyst, 2 equiv. of H_2O_2, room temperature and 20 mL of acetonitrile.

The recyclability of the catalyst was investigated by subjecting the beads to further 2 cycles under the same conditions. The results shown in Fig. 4 clearly show that the rate slows down after the first cycle, possibly indicating a change in coordination environment under the experimental conditions with further loss of activity on the third cycle possibly due to the leaching of the vanadium at the surface of the beads, which is in agreement with the AFM data. The results from the third cycle are comparable to those obtained with the 0.011 g amount of catalyst (see Fig. 1), once again supporting our argument about the loss of vanadium at the surfaces.

3.4.2. Oxidation of styrene

Fig. 5 shows the percentage conversions in the oxidation of styrene at different catalyst amounts using 2 equiv. of 30% H_2O_2. The reaction products that were identified by GC–MS are shown in Scheme 3.

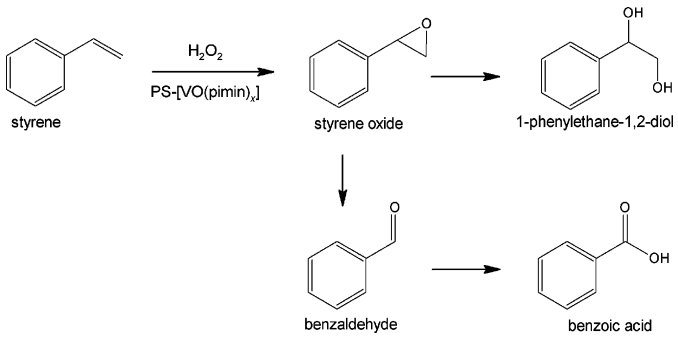

Scheme 3. Oxidation products from styrene.

The rates of conversion were very high at the beginning when the catalyst of 0.025 g or 0.035 g was used and rather slow when the catalyst of 0.011 g was used; however, the higher conversion of 83.9% was reached after 4 h compared with the former. It was therefore necessary to investigate the effect of oxidant since a maximum of 73% was reached within 2.5 h with 0.025 g of catalyst.

A maximum conversion of 99.5% was obtained with 4 equiv. of peroxide after only 2.5 h of reaction time, and surpassed the non-polymer-bound counterpart in initial rates (see Fig. 6). At two-equivalents of peroxide the initial rate of conversion for the homogeneous complex, [VO(pimin)$_2$], was comparable to that of the polymer-bound complex.

After 2.5 h, when the reaction reaches maximum conversion, the yield order is as follows: benzaldehyde (57.6%) > phenylethane-1,2-diol (16.2%) > benzoic acid (7.1%) and > styrene oxide (3.1%); clearly, styrene oxide converts readily to benzaldehyde and phenylethane-1,2-diol within that reaction time. It is only when benzaldehyde

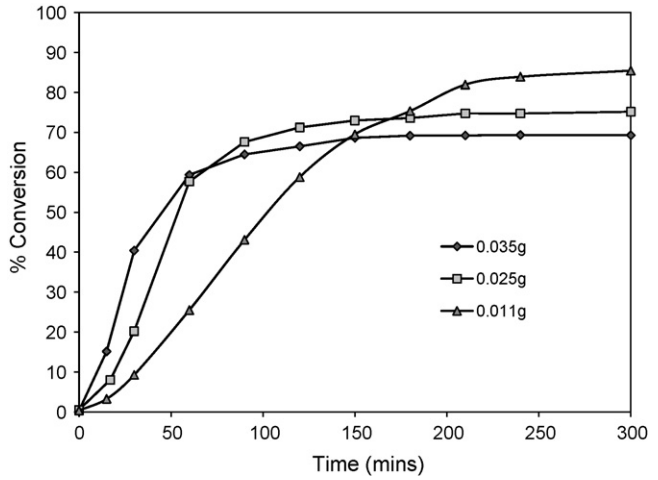

Fig. 5. The effect of catalyst amount on styrene oxidation. Reaction conditions: styrene (1.04 g, 10 mmol), 30% H_2O_2 (20 mmol), acetonitrile (20 mL) and 80 °C.

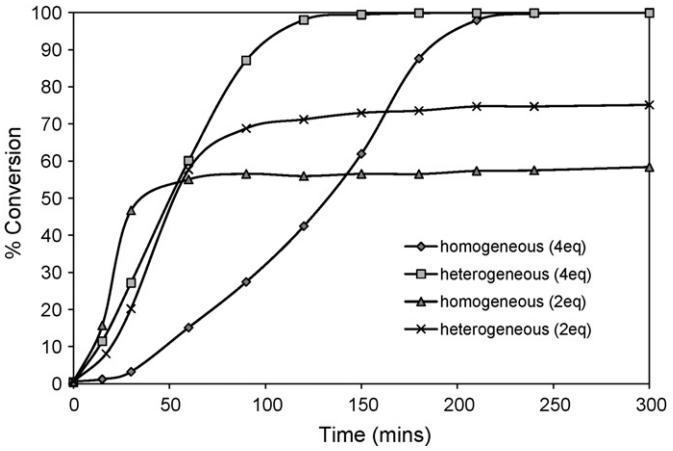

Fig. 6. Effect of the amount of oxidant on the oxidation of styrene (1.04 g) using 0.025 g of catalyst, and the comparison with neat complex (0.0090 g) at 80 °C and in 20 mL of acetonitrile.

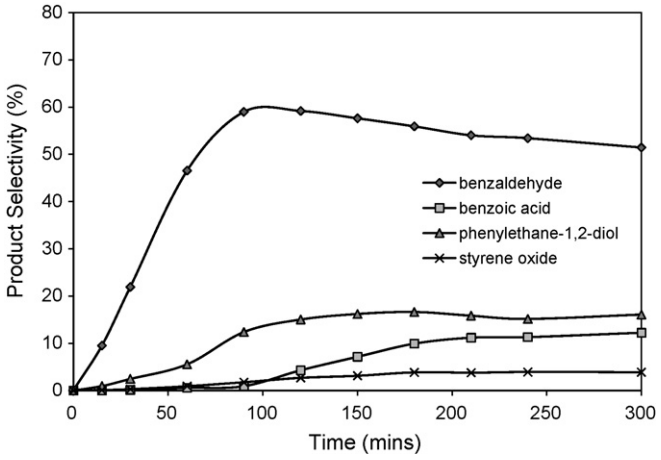

Fig. 7. Product selectivity for the oxidation of styrene. Reaction conditions: 1.04 g of styrene, 0.025 g of catalyst, 4 equiv. of H_2O_2, at 80 °C and 20 mL of acetonitrile.

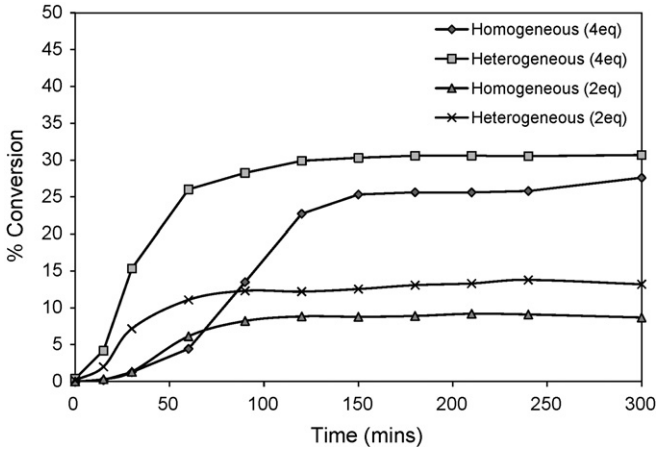

Fig. 8. Effect of the amount of oxidant on the oxidation of ethylbenzene (1.06 g) using 0.025 g of catalyst, and the comparison with neat complex (0.0090 g) at 80 °C and 20 mL of acetonitrile.

converts to benzoic acid that a steady state is reached for the conversion of styrene oxide (see Fig. 7).

3.4.3. Oxidation of ethylbenzene

Fig. 8 shows the effect of the peroxide-to-substrate ratio on the oxidation of ethylbenzene. A maximum conversion of 30.6% is obtained within 3 h of reaction time which is rather impressive for the oxidation of alkanes. The higher oxidant amount is crucial in achieving the highest conversion since the 2 equiv. amount of peroxide only yields a maximum of 13.1% within the same reaction time. The homogeneous analogue is once again inferior to PS-[VO(pimin)$_x$] in terms of activity under the same conditions for the oxidation of ethylbenzene.

The evidence of GC–MS and ^{1}H NMR data indicates that the main oxidation products for the oxidation of ethylbenzene were benzaldehyde and acetophenone (see Scheme 4).

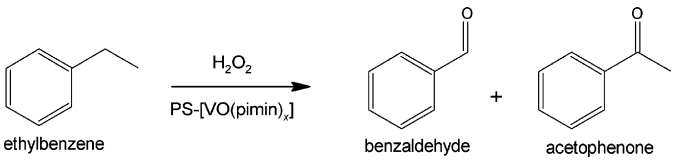

Scheme 4. The oxidation products from ethylbenzene.

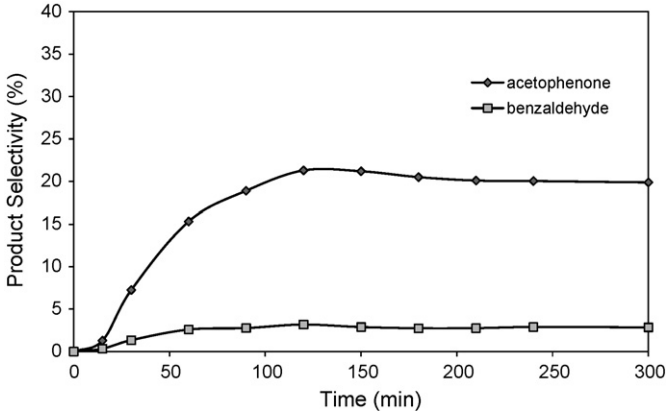

Fig. 9. Product selectivity for the oxidation of ethylbenzene. Reaction conditions: 1.06 g of ethylbenzene, 0.025 g of catalyst, 4 equiv. of H_2O_2, 80 °C and 20 mL of acetonitrile.

Table 2
Percentage conversion and turnover frequency (TOF).

Substrate	% conversion[a]	TOF (h^{-1})[b]	Catalyst amount (g)	H_2O_2 amount (mmol)	Temperature (°C)
Ethylbenzene	30.3	53	0.025[c]	40	80
Styrene	99.4	173	0.025[c]	40	80
Thioanisole	97.4	169	0.025[c]	20	RT
Thioanisole[d]	97.0	121	0.025[c]	20	RT
Thioanisole	98.8	860	0.025[c]	20	60
Ethylbenzene	25.3	31	0.009[e]	40	80
Styrene	99.8	78	0.009[e]	40	80
Thioanisole	98.6	613	0.009[e]	20	60

RT = room temperature.
[a] Maximum conversion of 10 mmol of substrate.
[b] Determined as moles of substrate converted/moles of vanadium in catalyst/time (h).
[c] Heterogeneous.
[d] Second cycle of catalyst.
[e] Homogeneous.

Fig. 9 shows that the conversion tends towards the formation of acetophenone with no trace of phenylacetic acid which was found earlier by other researchers [15]. At 3 h when a maximum is reached, the product selectivity order is acetophenone (20.5%) > benzaldehyde (2.7%).

The summary of the results of the oxidation reactions is presented in Table 2. The percentage conversions refer to the point of reaching a steady state and likewise for the turnover frequency. It is evident from these results that PS-[VO(pimin)$_x$] and to some extent its homogeneous analogue is most efficient in catalysing the oxidation of thioanisole.

3.4.4. Possible reaction pathways

When the beads are introduced to the reaction mixture, there is an immediate colour change from green to yellow, and this is attributed to the oxidation of the vanadium(IV) center. To provide insight into this first step of the mechanism, we have performed a titration of a solution of the complex (ca. 10^{-4} M), [VO(pimin)$_2$], with 30% hydrogen peroxide in dimethyl sulfoxide (DMSO). This reaction was monitored by electronic absorption spectroscopy (see Fig. 10). The disappearance of the three d–d transitions and the appearance of charge transfer band at 372 nm which appears as a shoulder of the n → π* band at 352 nm confirm this oxidation.

This spectral change is indicative of the formation of the oxoperoxovanadium(V) complex, which is the active intermediate species that participates in the oxidation reactions by transferring one of its oxygens to the substrate [15,21]. The induction periods

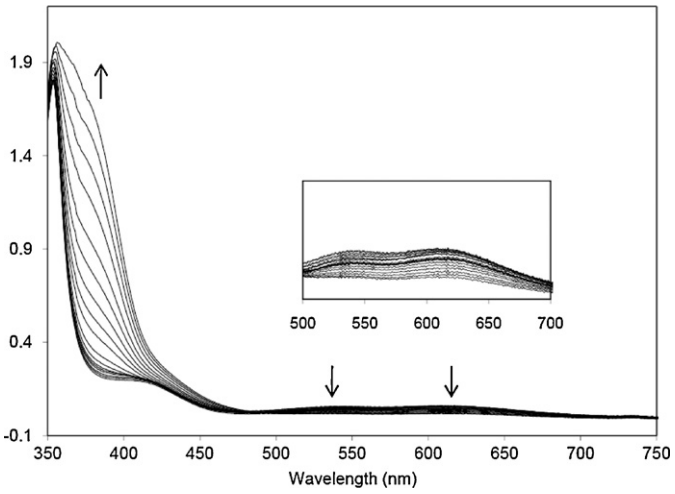

Fig. 10. Spectrophotometric titration of $[VO(pimin)_2]$ with H_2O_2 in DMSO.

observed in styrene and ethylbenzene oxidation reactions with PS-$[VO(pimin)_x]$ can be explained by this first step of the catalytic process. Generally, the induction periods for the homogeneous catalyst are longer than those for the heterogeneous catalyst but improve with a high oxidant amount. This delay is due to the activity of the different vanadyl centers which influence the rate of formation of oxoperoxovanadium(V) complex. This trend is not observed for thioanisole oxidation since sulfide oxidation with peroxide proceeds without delay in the absence of the catalyst (see Fig. 1).

The formation of styrene oxide from styrene has been discussed in detail by Mimoun et al. [22]. The dominant product for the oxidation of styrene in our case is benzaldehyde followed by phenylethane-1,2-diol and benzoic acid. This is not surprising since benzaldehyde can form from styrene oxide under acidic conditions by oxidative cleavage of the ring via a radical mechanism [21] while the water present in peroxide is responsible for the formation of phenylethane-1,2-diol [23]. The decrease in the benzaldehyde yield (Fig. 7) with reaction time seems to be influenced by the oxidation to benzoic acid in the presence of peroxide.

The oxidation of ethylbenzene yielded both benzaldehyde and acetophenone, with the latter being the major product. The mechanism of formation of acetophenone proposed by Hoshino et al. involves the abstraction of an α-hydrogen from ethylbenzene to form 1-phenylethyl radicals, followed by a reaction with oxygen to produce acetophenone. The formation of benzaldehyde is believed to occur via the decomposition of 1-phenylethoxyl radicals [24].

4. Conclusions

The polymer-anchored oxovanadium(IV) catalyst, PS-$[VO(pimin)_x]$, has been prepared. The catalytic activity for the oxidation of thioanisole, styrene and ethylbenzene has been evaluated by using 30% H_2O_2 as the oxidant. The catalyst showed good potential for the oxidation of the substrates, yielding the following conversions at the steady state; 99.6% for thioanisole (0.025 g of catalyst, RT and 2 equiv. of H_2O_2); and 99.9% and 30.6% respectively for styrene and ethylbenzene (0.025 g of catalyst, 80 °C and 2 equiv. of H_2O_2).

The resultant stereochemistry of the vanadium complex within the polymer was influenced by the alkylation of Hpimin to PS-Cl via the hydroxyl group yielding an ethereal connection rather than a nitrogen-bound ligand. This resulted in a cationic oxovanadium(IV) species forming within the polymer. The net result is that this catalyst degrades in the presence of high peroxide amount and at high temperatures. However, PS-$[VO(pimin)_x]$ should be suitable for room temperature oxidation of sulfides as shown by our AFM results and recyclability studies.

Acknowledgements

The authors would like to thank Mr M. Mtyopo from InnoVenton-Technology Support Unit (NMMU) for the GC–MS data, Dr. E. Antunes from DST/Mintek-NIC (Rhodes) for the microanalysis data and Dr. R. Nel from Sasol for supplying a fine temperature-regulating hotplate. We are also grateful for financial support from Sasol and NRF.

Appendix A. Supplementary data

Supplementary data associated with this article can be found, in the online version, at doi:10.1016/j.molcata.2009.11.004

References

[1] R. Ando, T. Yagyu, M. Maeda, Inorg. Chim. Acta 357 (2004) 2237–2244.
[2] D.C. Sherrington, Catal. Today 57 (2000) 87–104.
[3] S. Leinonen, D.C. Sherrington, A. Sneddon, D. McLoughlin, J. Corker, C. Canevali, F. Morazzoni, J. Reedijk, S.B.D. Spratt, J. Catal. 183 (1999) 251–266.
[4] M.M. Miller, D.C. Sherrington, J. Catal. 152 (1995) 368–376.
[5] D.C. Sherrington, Pure Appl. Chem. 60 (1987) 401–414.
[6] V. Conte, F. Di Furia, G. Licini, Appl. Catal. A 157 (1997) 335–361.
[7] S. Velusamy, A. Srinivasan, T. Punniyamurthy, Tetrahedron Lett. 47 (2006) 923–926.
[8] D. Bagchi, S.J. Stohs, B.W. Downs, M. Bagchi, H.G. Preuss, Toxicology 186 (2003) 175–177.
[9] C.L. Hill, T.M. Anderson, J.W. Han, D.A. Hillesheim, Y.V. Geletii, N.M. Okun, R. Cao, B. Botar, D.G. Musaev, K. Morokuma, J. Mol. Catal. A: Chem. 251 (2006) 234–238.
[10] S. Mohebbi, D.M. Boghaei, A.H. Sarvestani, A. Salimi, Appl. Catal. A 278 (2005) 263–267.
[11] P. Tau, T. Nyokong, J. Mol. Catal. A: Chem. 273 (2007) 149–155.
[12] V. Chauke, T. Nyokong, J. Mol. Catal. A: Chem. 289 (2008) 9–13.
[13] M.R. Maurya, A.K. Chandrakar, S. Chand, J. Mol. Catal. A: Chem. 274 (2007) 192–201.
[14] P. Paríк, S. Senauerová, V. Liková, K. Handlír, M. Ludwig, J. Heterocycl. Chem. 43 (2006) 835–841.
[15] M.R. Maurya, A. Arya, P. Adão, J.C. Pessoa, Appl. Catal. A 351 (2008) 239–252.
[16] C. Lü, B. Gao, Q. Liu, C. Qi, Colloid. Polym. Sci. 286 (2008) 553–561.
[17] T.J. Lane, I. Nakagawa, J.L. Walter, A.J. Kandathil, Inorg. Chem. 1 (1962) 267–276.
[18] J. Selbin, Chem. Rev. 65 (1965) 153–175.
[19] K.S. Patel, G.A. Kolawole, A. Earnshaw, J. Inorg. Nucl. Chem. 43 (1981) 3107–3112.
[20] M.R. Maurya, M. Kumar, A. Arya, Catal. Commun. 10 (2008) 187–191.
[21] M.R. Maurya, S. Sikarwar, M. Kumar, Catal. Commun. 8 (2007) 2017–2024.
[22] H. Mimoun, M. Mignard, P. Brechot, L. Saussine, J. Am. Chem. Soc. 108 (1986) 3711–3718.
[23] Z. Wang, Y.-T. Cui, Z.-B. Xu, J. Qu, J. Org. Chem. 73 (2008) 2270–2274.
[24] M. Hoshino, H. Akimoto, M. Okuda, Bull. Chem. Soc. Jpn. 51 (1978) 718–724.